Correlated Photon Dynamics in Dissipative Rydberg Media

Emil Zeuthen, Michael J. Gullans, Mohammad F. Maghrebi, and Alexey V. Gorshkov

Phys. Rev. Lett. **119**, 043602 — Published 26 July 2017

DOI: 10.1103/PhysRevLett.119.043602

Correlated photon dynamics in dissipative Rydberg media

Emil Zeuthen,[1,2,*] Michael J. Gullans,[3] Mohammad F. Maghrebi,[3] and Alexey V. Gorshkov[3]

[1]*Niels Bohr Institute, University of Copenhagen, DK-2100 Copenhagen, Denmark*
[2]*Institute for Theoretical Physics & Institute for Gravitational Physics (Albert Einstein Institute), Leibniz Universität Hannover, Callinstraße 38, 30167 Hannover, Germany*
[3]*Joint Quantum Institute and Joint Center for Quantum Information and Computer Science, National Institute of Standards and Technology and University of Maryland, College Park, Maryland 20742, USA*

Rydberg blockade physics in optically dense atomic media under the conditions of electromagnetically induced transparency (EIT) leads to strong dissipative interactions between single photons. We introduce a new approach to analyzing this challenging many-body problem in the limit of large optical depth per blockade radius. In our approach, we separate the single-polariton EIT physics from Rydberg-Rydberg interactions in a serialized manner while using a hard-sphere model for the latter, thus capturing the dualistic particle-wave nature of light as it manifests itself in dissipative Rydberg-EIT media. Using this approach, we analyze the saturation behavior of the transmission through one-dimensional Rydberg-EIT media in the regime of non-perturbative dissipative interactions relevant to current experiments. Our model is able to capture the many-body dynamics of bright, coherent pulses through these strongly interacting media. We compare our model with available experimental data in this regime and find good agreement. We also analyze a scheme for generating regular trains of single photons from continuous-wave input and derive its scaling behavior in the presence of imperfect single-photon EIT.

In optically dense atomic media, strong non-linear dissipative [1–6] and dispersive [7–9] inter-photon interactions at the single-quantum level can be engineered via interactions of hybrid atom-photon excitations called Rydberg polaritons [10, 11], propagating due to Electromagnetically Induced Transparency (EIT) [12]. Such photon-photon interactions can implement quantum gates between a pair of photons [13–15]; experimental realizations in this area include single-photon phase gates [16] and transistors [17, 18]. These interactions between photons can also lead to the generation of anti-bunched [4, 19] and other non-classical [6, 20–26] states of light.

The rich physics of dissipative Rydberg-EIT media and their potential as building blocks in quantum information science make urgent the challenge to understand the underlying quantum many-body dynamics. Whereas the few-photon theory has been established [4], a tractable approach for analyzing the high-intensity sector of interest to ongoing experiments [4, 27] has thus far not been available. In this Letter, we overcome these shortcomings by constructing a model for the many-body dynamics of one-dimensional dissipative Rydberg-EIT media. We compare our model with experimental data from Ref. [4] and find good agreement. We then show how this system can generate a regular train of single photons from uniform coherent-state input. Such photon trains have wide utility in applications such as boson sampling [28], quantum key distribution [29], and sub-shot-noise imaging of low-absorption samples [30]. At a more fundamental level, the emergence of a strongly correlated state of photons from a classical input is an interesting case study for emergent behavior in non-equilibrium quantum many-body systems.

In a simplistic picture of the high-intensity dynamics of such a medium [Fig. 1(a)], a bright continuous-wave

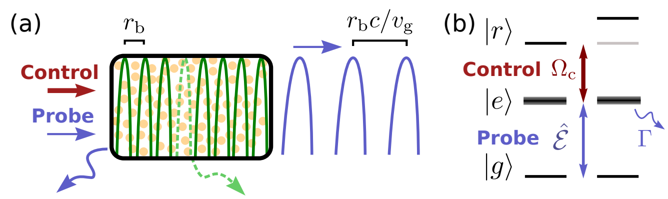

Figure 1. Dissipative Rydberg blockade in a one-dimensional atomic EIT medium. (a) Dynamics resulting from high-intensity CW probing according to naive expectation. The one-dimensional wave train of polaritons and outgoing photons is indicated. (b) Level diagram for the atoms leading to a dissipative blockade. Ground and Rydberg levels, $|g\rangle$ and $|r\rangle$, are long-lived compared to the lossy excited level $|e\rangle$ with decay rate 2Γ. Outside the blockade radius of Rydberg polaritons, an incoming photon enjoys EIT transmission (left set of energy levels). For atoms within the blockade region of a polariton, the Rydberg level $|r\rangle$ is shifted out of resonance with respect to the classical drive Ω_{c} causing an incoming photon to scatter out of the excited state $|e\rangle$.

(CW) probe field produces a train of Rydberg polaritons (green peaks). Via Rydberg-Rydberg (R-R) interactions, one polariton destroys lossless EIT-propagation conditions for other nearby polaritons. As a result, inside the medium, the polaritons are separated by their blockade radius r_{b} due to the scattering of "superfluous" photons at the entrance (purple wavy arrow) out of the forward-propagating mode. In turn, the polaritons exit the medium as a train of single photons spaced by the decompressed blockade radius $r_{\mathrm{b}}c/v_{\mathrm{g}}$ (v_{g} is the polariton group velocity and c is the speed of light). However, polaritons may decay (green dashed arrow) due to the finite width of the EIT window [4], whereby the observed anti-bunching feature will have an extent which significantly exceeds the blockade time $\tau_{\rm b} \equiv r_{\rm b}/v_{\rm g}$. This is due to the spectral features of width $\sim 1/\tau_{\rm b}$ generated by the blockade exceeding the bandwidth of the EIT transmission window. Consequently, these features are washed out due to EIT filtering and dispersion as the polaritons propagate through the medium. We include in our model these detrimental *single-polariton* EIT effects, that set the limits of control for Rydberg-EIT media, but have been ignored in existing theories for the high-intensity regime.

Rydberg-EIT blockade experiments have been performed in both free space [4, 31–34] and intra-cavity [35] settings. Focusing here on the former, a number of theoretical approaches to the dissipative blockade can be found in the literature: Theories based on semi-classical weak probing [36] and quantum super atoms [37–39], respectively, have both successfully predicted the experimental transmission data of Ref. [31]. Also accounting for the quantum nature of light, Ref. [13] analyzed the case of two strongly interacting photons. Here it was demonstrated that dissipative Rydberg-EIT media subject to copropagating input photons will produce an output field exhibiting the avoided volume associated with blockade, an effect that may serve as the basis of a single-photon filter in the limit of large optical depth per blockade radius $d_{\rm b} \gg 1$ [6].

Our model has two main advantages over previous work in this direction [6]: Firstly, by allowing for input pulses exceeding the blockade time $\tau_{\rm b}$, we can analyze the CW limit of operation. Secondly, we incorporate the fact that single-polariton EIT decay releases the blockade, thereby allowing for the formation of a new polariton.

To set up the model, we start by considering the limit of perfect single-polariton EIT, $d_{\rm b} \gg 1$, allowing us to discuss the R-R interactions independently. These arise in an ensemble of 3-level atoms in the ladder configuration [Fig. 1(b)], in which the van der Waals potential associated with a Rydberg excitation $|r\rangle$ tunes neighboring atoms out of the EIT condition, thus activating the dissipation channel of the excited state $|e\rangle$. For simplicity, we replace the potential by a hard-sphere potential of radius $r_{\rm b}$ such that inside this region the photons immediately scatter, whereas outside they are unaffected.

Within this hard-sphere model, the action of the Rydberg medium on a pulsed input can be understood as sketched in Fig. 2: If a photon successfully enters the medium, it forms a polariton propagating without loss at speed $v_{\rm g}$. If another photon enters at time $\tau_1 < \tau_{\rm b}$ after the polariton was created, it will scatter out of the forward-propagating mode. As a result, the environment effectively projects the wave function of the polariton to be localized within the arrival time interval $[\tau_1 - \tau_{\rm b}, \tau_1]$ [see Fig. 2(a)]. As long as the polariton is within the first blockade radius of the entrance, subsequent scattering events will not further localize the polariton [see Fig. 2(b)]; hence, only the single-polariton physics plays a role during the propagation through this region. Once the polariton has propagated a distance $r_{\rm b}$ into the medium, it can no longer cause scattering of incoming photons and a new polariton may be formed at the entrance of the medium [41]. When a polariton reaches the rear of the medium, it will map back onto the outgoing optical field after undergoing spatial decompression by a factor of $c/v_{\rm g}$.

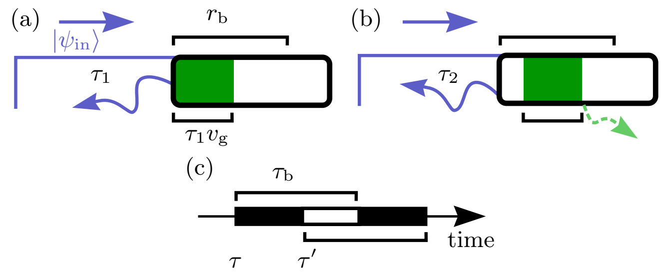

Figure 2. Formation of the polariton wave function by projection of an incoming pulse in state $|\psi_{\rm in}\rangle$ according to the hard-sphere model in the limit of perfect single-polariton EIT. (a) An incoming probe photon is scattered (purple wavy arrow) near the beginning of the medium at time τ_1 thereby creating a polariton pulse (green rectangle) in the medium. (b) This pulse propagates further into the medium until at a time τ_2 a second probe photon scatters, but since (in this instance) the polariton could not have left the first $r_{\rm b}$ of the medium, no additional projection of the polariton wave function ensues (see [40] for an extended discussion). The short duration of the polariton leads to EIT losses (green dashed arrow). (c) Geometrical derivation of polariton coherence: The overlap of the blockade regions during arrival times τ and τ' is indicated by shading. The "forbidden" region, during which scattering events would ruin the superposition between τ and τ', is shown in black (here assuming $|\tau - \tau'| \le \tau_{\rm b}$).

Dissipative theory at high intensity.—We will now apply these ideas to analyze two scenarios involving dissipative Rydberg-EIT media in the one-dimensional limit, where the transverse spot size of the impinging light fields is small compared to $r_{\rm b}$. As our first application, we consider the transmission behavior for a medium subject to CW probe and control fields as a function of the input rate $\mathcal{R}_{\rm in}$ of the probe.

Preliminarily, we derive the output rate in absence of single-polariton EIT decay, i.e., only considering the R-R interaction. The input rate $\mathcal{R}_{\rm in}$ splits into two fractions, the rate of photons that make it through the medium $\mathcal{R}_{\rm out}$ and a rate of R-R scattered photons, $\mathcal{R}_{\rm out}\tau_{\rm b}\mathcal{R}_{\rm in}$ [42]:

$$\mathcal{R}_{\rm in} = \mathcal{R}_{\rm out} + \mathcal{R}_{\rm out}\tau_{\rm b}\mathcal{R}_{\rm in}; \qquad (1)$$

$\tau_{\rm b}\mathcal{R}_{\rm in}$ is the average number of photons scattered by each Rydberg polariton, while $\mathcal{R}_{\rm out}$ is the rate of periods where the medium is blockaded. From Eq. (1), we find the desired result [43]

$$\mathcal{R}_{\rm out} = \frac{1}{\tau_{\rm b} + 1/\mathcal{R}_{\rm in}}. \tag{2}$$

As expected, the output rate $\mathcal{R}_{\rm out}$ is upper-bounded by both the input rate $\mathcal{R}_{\rm in}$ and the inverse blockade time $1/\tau_{\rm b}$, with each bound achievable in the limit of weak blockade $\tau_{\rm b} \to 0$ and high input rate $\mathcal{R}_{\rm in} \to \infty$, respectively.

We now turn to the more realistic case of imperfect single-polariton EIT, in which we must account for the finite transmission of polaritons that do not fit within the EIT window. If a polariton is EIT-scattered within the first blockade radius $r_{\rm b}$ of the medium, its blockading effect ceases, hence allowing for the creation of a new polariton at the input of the medium. Therefore the average blockade time per polariton $\bar{\tau}_{\rm b}$ is upper-bounded by that of a polariton that makes it through the first $r_{\rm b}$ of the medium, $\bar{\tau}_{\rm b} \le \tau_{\rm b}$. Introducing the average single-polariton EIT transmission $\bar{\eta}_{\rm EIT}(L)$ through a medium of length $L \ge r_{\rm b}$ and the average Rydberg formation rate $\mathcal{R}_{\rm Rf}$, we decompose the input rate in the spirit of Eq. (1),

$$\mathcal{R}_{\rm in} = \bar{\eta}_{\rm EIT}(L)\mathcal{R}_{\rm Rf} + [1-\bar{\eta}_{\rm EIT}(L)]\mathcal{R}_{\rm Rf} + \mathcal{R}_{\rm Rf}\bar{\tau}_{\rm b}\mathcal{R}_{\rm in}, \tag{3}$$

where on the right-hand side the first term is the output rate, $\mathcal{R}_{\rm out} \equiv \bar{\eta}_{\rm EIT}(L)\mathcal{R}_{\rm Rf}$, the second term is the rate of polariton EIT decay, and the third term is the rate of R-R scattering events. Introducing the output rate $\mathcal{R}_{\rm out}$ into Eq. (3) and solving for this quantity, we find

$$\mathcal{R}_{\rm out} = \frac{\bar{\eta}_{\rm EIT}(L)}{\bar{\tau}_{\rm b} + 1/\mathcal{R}_{\rm in}}, \tag{4}$$

generalizing Eq. (2). Equation (4) shows that EIT decay alters the transmission not only by the trivial damping prefactor $\bar{\eta}_{\rm EIT}$, but also by decreasing the effective blockade time $\bar{\tau}_{\rm b} \le \tau_{\rm b}$. Moreover, since both $\bar{\eta}_{\rm EIT}$ and $\bar{\tau}_{\rm b}$ are likely to decrease with increasing $\mathcal{R}_{\rm in}$, the transmission curve (4) need not be a monotonous function of $\mathcal{R}_{\rm in}$.

To evaluate Eq. (4), we estimate $\bar{\eta}_{\rm EIT}(L)$ and $\bar{\tau}_{\rm b}$ using the idea of projection-free propagation discussed in connection with Fig. 2(a,b). This allows a serialized treatment: We take the temporal extent τ of a polariton to be defined by the first R-R event after its formation and average over the Poisson distribution for the arrival times of photons. The associated EIT transmission is then modeled by that of a square pulse of duration τ subjected to Gaussian filtering, yielding the following expressions [40],

$$\bar{\eta}_{\rm EIT}(l) = \exp\left([\tau_{\rm EIT}(l)\mathcal{R}_{\rm in}]^2\right) {\rm erfc}\left(\tau_{\rm EIT}(l)\mathcal{R}_{\rm in}\right), \tag{5}$$

$$\frac{\bar{\tau}_{\rm b}}{\tau_{\rm b}} = \int_0^{r_{\rm b}} \frac{dl}{r_{\rm b}} \bar{\eta}_{\rm EIT}(l) = \frac{\bar{\eta}_{\rm EIT}(r_{\rm b}) + \sqrt{\frac{4}{\pi}}\tau_{\rm EIT}(r_{\rm b})\mathcal{R}_{\rm in} - 1}{[\tau_{\rm EIT}(r_{\rm b})\mathcal{R}_{\rm in}]^2}, \tag{6}$$

where the full blockade time is $\tau_{\rm b} = d_{\rm b}/(2\gamma_{\rm EIT})$, the filtering time $\tau_{\rm EIT}(l) \equiv \sqrt{d_{\rm b} l/r_{\rm b}}/\gamma_{\rm EIT}$ and $\gamma_{\rm EIT} \equiv \Omega_{\rm c}^2/\Gamma$ is the single-atom EIT linewidth in terms of the control field Rabi frequency $\Omega_{\rm c}$ and the halfwidth Γ of the intermediate level [44]; taken together with these definitions, Eqs. (5,6) determine the output rate (4).

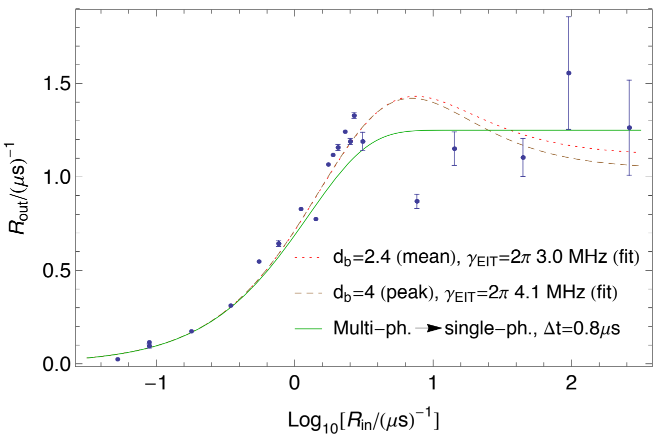

Figure 3. Transmission through a dissipative Rydberg-EIT medium. Output rate $\mathcal{R}_{\rm out}$ as function of input rate $\mathcal{R}_{\rm in}$. The data from Ref. [4] is compared to plots of Eq. (4) for two fixed values of $d_{\rm b}$ corresponding to mean (red dotted) and peak (brown dashed) values of the Gaussian atomic density distribution in the experiment with axial spread $\sigma_{\rm ax}$ and with effective length $L = 4.2 \times \sigma_{\rm ax}$. The value for the single-atom EIT linewidth in the experiment was $\gamma_{\rm EIT} = 2\pi \times 7.5$ MHz. Also plotted (solid green curve) is the rate resulting from converting all multi-photon events within successive time intervals $\Delta t = 0.8\,\mu$s into single-photon events $\mathcal{R}_{\rm out} = (\Delta t)^{-1}(1-e^{-\mathcal{R}_{\rm in}\Delta t})$. The latter was presented alongside the data in Ref. [4].

We plot Eq. (4) in Fig. 3 using the experimental parameters of Ref. [4] and compare to the data and the alternative theoretical curve presented therein (however, $\gamma_{\rm EIT}$ was obtained by fitting Eq. (4) to the data resulting in values within a factor of 2 from that cited in Ref. [4]). Within the error bars of the data, Eq. (4) is seen to match the data equally well as the theoretical curve proposed in Ref. [4]. Crucially, however, the physics implicit in the latter functional form is at odds with that of the Rydberg blockade: It puts no lower limit on the spacing between output photons, and the time-scale Δt that must be assumed to fit the data is an order of magnitude larger than $\tau_{\rm b}$ calculated from experimental parameters. Eq. (4) predicts the following two features of the transmission curve: Firstly, a finite asymptote for the limit of very high intensity, $\mathcal{R}_{\rm in} \to \infty$; while in this limit the average transmission probability goes to zero, $\bar{\eta}_{\rm EIT}(L) \to 0$, the effective blockade time will likewise decrease, $\bar{\tau}_{\rm b} \to 0$, thereby increasing the polariton formation rate in a manner such that $\mathcal{R}_{\rm out}$ in Eq. (4) remains finite. Secondly, Eq. (4) in general exhibits a local maximum as in Fig. 3.

Generation of a single-photon train.—We will now show that, in the limit $d_{\rm b} \gg 1$, a CW probe gets con-

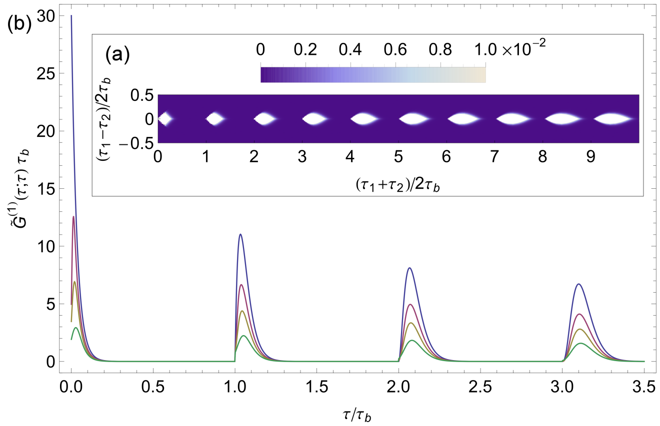

Figure 4. (a) $G^{(1)}(\tau_1;\tau_2)$ [in units of $1/\tau_\mathrm{b}$] for coherent square-pulse input entering the medium at $\tau = 0$ in the limit of perfect single-polariton EIT, Eq. (8) with $\mathcal{R}_\mathrm{in} = 30/\tau_\mathrm{b}$ (values $> 10^{-2}$ are plotted as white for illustrative purposes). (b) Diagonal elements of the EIT-filtered correlation function $\tilde{G}^{(1)}(\tau;\tau)$ for EIT width $1/\tau_\mathrm{EIT}$, where $\tau_\mathrm{EIT}\mathcal{R}_\mathrm{in} \in \{0, 1/4, 1/2, 1\}$ (in order of decreasing amplitude: purple, magenta, yellow, green).

verted into a regular pulse train of single photons [see Fig. 1(a)]. The blockade sets a lower limit τ_b to the temporal separation of output photons leading to antibunching. To achieve regularity, we must also impose an upper bound on the (average) separation. This can be ensured by a sufficiently large input rate, but only insofar as single-polariton EIT decay remains rare. Such a decay event will terminate the regularity of the pulse train (creating a "domain wall"), effectively resetting the process. These considerations imply that an optimum input rate exists as a trade-off between the input photons not being too far apart (on average) while keeping single-polariton EIT decay at a perturbative level. In this regime, we may take $\bar{\tau}_\mathrm{b} \approx \tau_\mathrm{b}$ and estimate $\bar{\eta}_\mathrm{EIT}$ by filtering the correlation functions $G^{(1)}(\tau;\tau')$ produced by the idealized R-R interaction [see Fig. 2(a,b)] (as was checked by numerical simulations [40]).

We first derive the diagonal element $G^{(1)}(\tau;\tau)$ by observing that its value at a time τ after the onset of the pulse can have contributions from at most $\lceil \tau/\tau_\mathrm{b} \rceil$ polaritons per the hard-sphere ansatz. The contribution from each polariton follows from straightforward integration of the Poisson distribution; we then find ($\tau \geq 0$) [40]

$$G^{(1)}(\tau;\tau) = \sum_{j=0}^{\lfloor \tau/\tau_\mathrm{b} \rfloor} \mathcal{R}_\mathrm{in} e^{-\mathcal{R}_\mathrm{in}(\tau - j\tau_\mathrm{b})} \frac{[\mathcal{R}_\mathrm{in}(\tau - j\tau_\mathrm{b})]^j}{j!} \quad (7)$$

(the argument can be extended to obtain higher-order correlation functions [40]). This function is plotted in Fig. 4(b) (top blue curve) in the high-intensity regime in which the statistical uncertainty in the creation time of polaritons is small (relative to τ_b); i.e., when only the term $j = \lfloor \tau/\tau_\mathrm{b} \rfloor$ in Eq. (7) contributes significantly.

The first-order correlation function $G^{(1)}(\tau;\tau') = \langle \hat{\mathcal{E}}^\dagger(\tau)\hat{\mathcal{E}}(\tau')\rangle$ quantifies the quantum coherence between having a Rydberg excitation at different times. This can be related to the diagonal elements $G^{(1)}(\tau'';\tau'')$ by noting that $G^{(1)}(\tau;\tau')$ is the probability density for the creation of a polariton at time $\tau_< \equiv \min\{\tau,\tau'\}$ multiplied by the probability that no scattering events occur that allow the environment to distinguish whether the polariton was created at τ or τ'. From Fig. 2(c) we see that this requires that no photons impinge on the medium for intervals of combined duration $2|\tau-\tau'|$ [45], which is all the information needed for Poisson-distributed input (here focusing on $|\tau-\tau'| \leq \tau_\mathrm{b}$ relevant for the limit of interest, $d_\mathrm{b} \gg 1$, in which $\tau_\mathrm{EIT} \ll \tau_\mathrm{b}$). Hence ($|\tau-\tau'| \leq \tau_\mathrm{b}$)

$$G^{(1)}(\tau;\tau') = G^{(1)}(\tau_<;\tau_<)e^{-2\mathcal{R}_\mathrm{in}|\tau-\tau'|}, \quad (8)$$

where the diagonal elements of $G^{(1)}$ are given by Eq. (7). Equation (8) is plotted in Fig. 4(a). By convolving Eq. (8) with a Gaussian filter function corresponding to a medium of length $L = r_\mathrm{b}$, we estimate the effect of EIT decay, obtaining the intensity profile $\tilde{G}^{(1)}(\tau;\tau)$ plotted in Fig. 4(b).

Equation (7) captures how the accumulated randomness in the photon arrival times determines the spread in the formation times of polaritons. To obtain a parameter condition ensuring regularity of the pulse train for the first N_loc peaks of $G^{(1)}(\tau;\tau')$, we demand that the width $(\delta t)_N$ of the widest peak in the train obeys $(\delta t)_N \leq \beta\tau_\mathrm{b}$ for some fraction β of τ_b, yielding the requirement ($N_\mathrm{loc} \gg 1$) $\mathcal{R}_\mathrm{in} \gtrsim \sqrt{N_\mathrm{loc}}/(\beta\tau_\mathrm{b})$ [40]. On the other hand, if we can tolerate an EIT loss fraction of at most $\epsilon = 1-\bar{\eta}_\mathrm{EIT}$, filtering Eq. (8) yields an upper bound (in the limit $\tau_\mathrm{EIT} \ll 1/\mathcal{R}_\mathrm{in}, \tau_\mathrm{b}$), $\mathcal{R}_\mathrm{in} \lesssim 1/(N_\mathrm{EIT}\tau_\mathrm{EIT})$, where $N_\mathrm{EIT} \sim 1/\epsilon$ is the average pulse train length allowed by the EIT filter. Balancing these two considerations by setting $N = N_\mathrm{loc} = N_\mathrm{EIT}$ and seeking its maximal value N_max that permits the simultaneous fulfillment of the above requirements, we find

$$N_\mathrm{max} \sim \sqrt[3]{\frac{\pi\beta^2}{128\ln 2}d_\mathrm{b}}, \quad (9)$$

having used $\tau_\mathrm{b} = d_\mathrm{b}/(2\gamma_\mathrm{EIT})$ and $\tau_\mathrm{EIT} = \sqrt{d_\mathrm{b}}/\gamma_\mathrm{EIT}$. For this expression to reach $N_\mathrm{max} \gtrsim 1$ requires $d_\mathrm{b} \gtrsim 100$ for $\beta \approx 1/2$ and hence we find the generation of single-photon pulse trains to demand very large d_b. The scaling behavior (9) resulting from the limiting effects identified here may be improved by directing the scattered light into well defined channels using cooperative light emission [46].

In conclusion, we have proposed a new model for analyzing the many-body physics of the dissipative Rydberg blockade in extended one-dimensional EIT media. The work presented here may serve as a guide for the rigorous derivation of effective many-body theories [47]. In this regard, we remark that ongoing work on numerically simulating Rydberg-EIT media using matrix product states yields results which are in qualitative agreement with the present work [48, 49].

One can envision several extensions of our approach: Storage and retrieval operations in Rydberg media can be modeled by translating time-varying control fields into a time-dependent blockade time τ_b of hard-sphere Rydberg polaritons. In three-dimensional Rydberg media, multi-body Rydberg scattering events can take place when the blockade regions of transversely spaced polaritons overlap. It would also be intriguing to consider whether our protocol for the generation of photon trains can be modified, perhaps by employing cooperative resonances in regular atomic arrays [50], to turn the photon trains into time crystals [51, 52] that keep their periodicity for times that are exponentially long in the input intensity.

EZ is grateful to J. Taylor and the JQI for hosting him during the time when this project was conceived. We thank the Vuletić-Lukin group for providing their experimental data. We thank Q.-Y. Liang, J. Thompson, V. Vuletić, M. Lukin, J. Taylor, O. Firstenberg, T. Pohl, C. Murray, S. Hofferberth, D. Chang, N. Yao, and C. Nayak for discussions. EZ acknowledges funding from the European Research Council under the European Union's Seventh Framework Programme (FP/2007-2013) / ERC Grant Agreement n. 306576. MJG, MFM, and AVG thank the following funding sources: ARL CDQI, NSF QIS, NSF PFC at JQI, AFOSR, ARO, and ARO MURI. W. H. P. Nielsen provided graphical assistance.

---

* zeuthen@nbi.ku.dk

[1] J. D. Pritchard, D. Maxwell, A. Gauguet, K. J. Weatherill, M. P. A. Jones, and C. S. Adams, "Cooperative atom-light interaction in a blockaded rydberg ensemble," Phys. Rev. Lett. **105**, 193603 (2010).

[2] David Petrosyan, Johannes Otterbach, and Michael Fleischhauer, "Electromagnetically induced transparency with rydberg atoms," Phys. Rev. Lett. **107**, 213601 (2011).

[3] Y. O. Dudin and A. Kuzmich, "Strongly interacting rydberg excitations of a cold atomic gas," Science **336**, 887–889 (2012).

[4] Thibault Peyronel, Ofer Firstenberg, Qi-Yu Liang, Sebastian Hofferberth, Alexey V. Gorshkov, Thomas Pohl, Mikhail D. Lukin, and Vladan Vuletic, "Quantum nonlinear optics with single photons enabled by strongly interacting atoms," Nature **488**, 57–60 (2012).

[5] D. Maxwell, D. J. Szwer, D. Paredes-Barato, H. Busche, J. D. Pritchard, A. Gauguet, K. J. Weatherill, M. P. A. Jones, and C. S. Adams, "Storage and control of optical photons using rydberg polaritons," Phys. Rev. Lett. **110**, 103001 (2013).

[6] Alexey V. Gorshkov, Rejish Nath, and Thomas Pohl, "Dissipative many-body quantum optics in rydberg media," Phys. Rev. Lett. **110**, 153601 (2013).

[7] Ofer Firstenberg, Thibault Peyronel, Qi-Yu Liang, Alexey V. Gorshkov, Mikhail D. Lukin, and Vladan Vuletic, "Attractive photons in a quantum nonlinear medium," Nature (London) **502**, 71 (2013).

[8] P. Bienias, S. Choi, O. Firstenberg, M. F. Maghrebi, M. Gullans, M. D. Lukin, A. V. Gorshkov, and H. P. Büchler, "Scattering resonances and bound states for strongly interacting rydberg polaritons," Phys. Rev. A **90**, 053804 (2014).

[9] M. F. Maghrebi, M. J. Gullans, P. Bienias, S. Choi, I. Martin, O. Firstenberg, M. D. Lukin, H. P. Büchler, and A. V. Gorshkov, "Coulomb bound states of strongly interacting photons," Phys. Rev. Lett. **115**, 123601 (2015).

[10] M. D. Lukin, M. Fleischhauer, R. Cote, L. M. Duan, D. Jaksch, J. I. Cirac, and P. Zoller, "Dipole blockade and quantum information processing in mesoscopic atomic ensembles," Phys. Rev. Lett. **87**, 037901 (2001).

[11] Daniel Comparat and Pierre Pillet, "Dipole blockade in a cold rydberg atomic sample [invited]," J. Opt. Soc. Am. B **27**, A208–A232 (2010).

[12] Michael Fleischhauer, Atac Imamoglu, and Jonathan P. Marangos, "Electromagnetically induced transparency: Optics in coherent media," Rev. Mod. Phys. **77**, 633–673 (2005).

[13] Alexey V. Gorshkov, Johannes Otterbach, Michael Fleischhauer, Thomas Pohl, and Mikhail D. Lukin, "Photon-photon interactions via rydberg blockade," Phys. Rev. Lett. **107**, 133602 (2011).

[14] Ephraim Shahmoon, Gershon Kurizki, Michael Fleischhauer, and David Petrosyan, "Strongly interacting photons in hollow-core waveguides," Phys. Rev. A **83**, 033806 (2011).

[15] D. Paredes-Barato and C. S. Adams, "All-optical quantum information processing using rydberg gates," Phys. Rev. Lett. **112**, 040501 (2014).

[16] Daniel Tiarks, Steffen Schmidt, Gerhard Rempe, and Stephan Dürr, "Optical π phase shift created with a single-photon pulse," Sci. Adv. **2**, e1600036–e1600036 (2016).

[17] Daniel Tiarks, Simon Baur, Katharina Schneider, Stephan Dürr, and Gerhard Rempe, "Single-Photon Transistor Using a Förster Resonance," Phys. Rev. Lett. **113**, 053602 (2014).

[18] H Gorniaczyk, C Tresp, J Schmidt, H Fedder, and S Hofferberth, "Single-photon transistor mediated by interstate Rydberg interactions," Phys. Rev. Lett. **113**, 053601 (2014).

[19] D. Maxwell, D. J. Szwer, D. Paredes-Barato, H. Busche, J. D. Pritchard, A. Gauguet, M. P. A. Jones, and C. S. Adams, "Microwave control of the interaction between two optical photons," Phys. Rev. A **89**, 043827 (2014).

[20] Anne E. B. Nielsen and Klaus Mølmer, "Deterministic multimode photonic device for quantum-information processing," Phys. Rev. A **81**, 043822 (2010).

[21] T. Pohl, E. Demler, and M. D. Lukin, "Dynamical crystallization in the dipole blockade of ultracold atoms," Phys. Rev. Lett. **104**, 043002 (2010).

[22] F. Bariani, Y. O. Dudin, T. A. B. Kennedy, and A. Kuzmich, "Dephasing of multiparticle rydberg excitations for fast entanglement generation," Phys. Rev. Lett. **108**, 030501 (2012).

[23] J. D. Pritchard, C. S. Adams, and K. Mølmer, "Correlated photon emission from multiatom rydberg dark states," Phys. Rev. Lett. **108**, 043601 (2012).

[24] Jovica Stanojevic, Valentina Parigi, Erwan Bimbard,

Alexei Ourjoumtsev, Pierre Pillet, and Philippe Grangier, "Generating non-gaussian states using collisions between rydberg polaritons," Phys. Rev. A **86**, 021403 (2012).
[25] A Grankin, E Brion, E Bimbard, R Boddeda, I Usmani, A Ourjoumtsev, and P Grangier, "Quantum statistics of light transmitted through an intracavity rydberg medium," New Journal of Physics **16**, 043020 (2014).
[26] Mohammad F. Maghrebi, Norman Y. Yao, Mohammad Hafezi, Thomas Pohl, Ofer Firstenberg, and Alexey V. Gorshkov, "Fractional quantum hall states of rydberg polaritons," Phys. Rev. A **91**, 033838 (2015).
[27] S. Hofferberth, Private communication.
[28] Keith R. Motes, Alexei Gilchrist, Jonathan P. Dowling, and Peter P. Rohde, "Scalable boson sampling with timebin encoding using a loop-based architecture," Phys. Rev. Lett. **113**, 120501 (2014).
[29] P. Zoller, T. Beth, D. Binosi, R. Blatt, H. Briegel, D. Bruss, T. Calarco, J. I. Cirac, D. Deutsch, J. Eisert, A. Ekert, C. Fabre, N. Gisin, P. Grangiere, M. Grassl, S. Haroche, A. Imamoglu, A. Karlson, J. Kempe, L. Kouwenhoven, S. Kroll, G. Leuchs, M. Lewenstein, D. Loss, N. Lutkenhaus, S. Massar, J. E. Mooij, M. B. Plenio, E. Polzik, S. Popescu, G. Rempe, A. Sergienko, D. Suter, J. Twamley, G. Wendin, R. Werner, A. Winter, J. Wrachtrup, and A. Zeilinger, "Quantum information processing and communication - strategic report on current status, visions and goals for research in europe," Eur. Phys. J. D **36**, 203 (2005).
[30] G. Brida, M. Genovese, and I. Ruo Berchera, "Experimental realization of sub-shot-noise quantum imaging," Nat Photon **4**, 227 (2010).
[31] J. D. Pritchard, D. Maxwell, A. Gauguet, K. J. Weatherill, M. P. A. Jones, and C. S. Adams, "Cooperative atom-light interaction in a blockaded rydberg ensemble," Phys. Rev. Lett. **105**, 193603 (2010).
[32] Y. O. Dudin and A. Kuzmich, "Strongly interacting rydberg excitations of a cold atomic gas," Science **336**, 887–889 (2012).
[33] D. Maxwell, D. J. Szwer, D. Paredes-Barato, H. Busche, J. D. Pritchard, A. Gauguet, K. J. Weatherill, M. P. A. Jones, and C. S. Adams, "Storage and control of optical photons using rydberg polaritons," Phys. Rev. Lett. **110**, 103001 (2013).
[34] C. S. Hofmann, G. Günter, H. Schempp, M. Robert-de-Saint-Vincent, M. Gärttner, J. Evers, S. Whitlock, and M. Weidemüller, "Sub-poissonian statistics of rydberg-interacting dark-state polaritons," Phys. Rev. Lett. **110**, 203601 (2013).
[35] R Boddeda, I Usmani, E Bimbard, A Grankin, A Ourjoumtsev, E Brion, and P Grangier, "Rydberg-induced optical nonlinearities from a cold atomic ensemble trapped inside a cavity," Journal of Physics B: Atomic, Molecular and Optical Physics **49**, 084005 (2016).
[36] S. Sevinçli, N. Henkel, C. Ates, and T. Pohl, "Nonlocal nonlinear optics in cold rydberg gases," Phys. Rev. Lett. **107**, 153001 (2011).
[37] David Petrosyan, Johannes Otterbach, and Michael Fleischhauer, "Electromagnetically induced transparency with rydberg atoms," Phys. Rev. Lett. **107**, 213601 (2011).
[38] Yi-Mou Liu, Dong Yan, Xue-Dong Tian, Cui-Li Cui, and Jin-Hui Wu, "Electromagnetically induced transparency with cold rydberg atoms: Superatom model beyond the weak-probe approximation," Phys. Rev. A **89**, 033839 (2014).
[39] Martin Gärttner, Shannon Whitlock, David W. Schönleber, and Jörg Evers, "Semianalytical model for nonlinear absorption in strongly interacting rydberg gases," Phys. Rev. A **89**, 063407 (2014).
[40] See the Supplemental Material.
[41] Generally, this will lead to entanglement between polaritons and, hence, between the outgoing photons as discussed in the Supplemental Material.
[42] We neglect finite-pulse corrections that arise from a finite averaging time.
[43] Jörg W. Müller, "Some formulae for a dead-time-distorted poisson process: To andré allisy on the completion of his first half century," Nuclear Instruments and Methods **117**, 401 – 404 (1974).
[44] $\tau_{\rm EIT}$ is the inverse Gaussian width of the EIT amplitude filtering $\propto \exp(-\omega^2\tau_{\rm EIT}^2/2)$ and the convention for $\Omega_{\rm c}$ is set by $\partial_t\hat{P} = i\Omega_{\rm c}\hat{S}$, where $\hat{P}$ and $\hat{S}$ are the polarizations between $|g\rangle$–$|e\rangle$ and $|g\rangle$–$|r\rangle$ transitions, respectively.
[45] Assuming $\tau, \tau' \leq \tau_{\rm p} - \tau_{\rm b}$, where $\tau_{\rm p}$ is the pulse duration.
[46] C. R. Murray and T. Pohl, "Coherent photon manipulation in interacting atomic ensembles," ArXiv e-prints (2017), arXiv:1702.03763 [quant-ph].
[47] M. J. Gullans, J. D. Thompson, Y. Wang, Q.-Y. Liang, V. Vuletić, M. D. Lukin, and A. V. Gorshkov, "Effective field theory for rydberg polaritons," Phys. Rev. Lett. **117**, 113601 (2016).
[48] M. T. Manzoni, D. E. Chang, and J. S. Douglas, "Simulating quantum light propagation through atomic ensembles using matrix product states," ArXiv e-prints (2017), arXiv:1702.05954 [quant-ph].
[49] J. S. Douglas et al., In preparation.
[50] Ephraim Shahmoon, Dominik S. Wild, Mikhail D. Lukin, and Susanne F. Yelin, "Cooperative resonances in light scattering from two-dimensional atomic arrays," arXiv:1610.00138 (2016).
[51] Frank Wilczek, "Quantum time crystals," Phys. Rev. Lett. **109**, 160401 (2012).
[52] Alfred Shapere and Frank Wilczek, "Classical time crystals," Phys. Rev. Lett. **109**, 160402 (2012).